J Fusion Energ (2016) 35:694–701
DOI 10.1007/s10894-016-0092-z

ORIGINAL RESEARCH

Deuterium Plasma Focus as a Tool for Testing Materials of Plasma Facing Walls in Thermonuclear Fusion Reactors

M. Akel[1] · S. Alsheikh Salo[1] · Sh. Ismael[1] · S. H. Saw[2,3] · S. Lee[2,4,5]

Published online: 21 April 2016

Abstract This paper presents the first verification of the fast ion beam (FIB) and fast plasma stream (FPS) properties computed using the Lee code. Recent estimates of FIB and FPS properties in PF-400J from interferometric images are compared to our computed results. Reasonable agreement is found in the comparison of several quantities. Our computed power flow density (energy flux) and integral damage factor are 2.45×10^{12} Wm^{-2} (2 times of experimental value) and 1.78×10^{8} Wm^{-2} $s^{0.5}$ (~almost the same as experimental value) respectively, for target placed at 1.5 cm from the anode top of PF-400J. This verification gives us confidence to proceed to systematic numerical calculations on the PF-400J and similar small plasma focus devices (PF50, NX2, NX3, FMPF-3, INTI PF) to obtain FIB properties (ion beam energy, ion beam flux, ion beam fluence, beam ion number, ion beam current, power flow density, and damage factor). These results confirm that the plasma focus, including small ones, could be useful to study the effects of cumulative pulses on target materials being considered for plasma facing walls in future tokamak or laser-implosion fusion reactors.

✉ M. Akel
pscientific@aec.org.sy

[1] Department of Physics, Atomic Energy Commission, P. O. Box 6091, Damascus, Syria

[2] Institute for Plasma Focus Studies, 32 Oakpark Drive, Chadstone, VIC 3148, Australia

[3] Nilai University, 1, Persiaran Universiti, Putra Nilai, 71800 Nilai, Malaysia

[4] Physics Department, University of Malaya, Kuala Lumpur, Malaysia

[5] INTI International University, 71800 Nilai, Malaysia

Keywords Ion beam properties · Plasma focus · Lee model · Fusion wall materials · Damage factors

Introduction

A Plasma Focus (PF) is a pinch device in which a high-pulsed voltage is applied to a low-pressure gas, between coaxial cylindrical electrodes, generating a short-duration high-density plasma region in the axis (pinch) during the radial phase. Plasma focus pinches produce radiation pulses (neutrons and X-rays), shock waves, ions and electron beams, plasma filaments, plasma jets, and plasma bursts, being an interesting plasma accelerator to study the effects of fusion-relevant pulses on materials. In effect, targets of different materials relevant to fusion reactors can be characterized using the plasma focus environment (using single pulses, or several cumulative pulses), which can simulate conditions similar to those that will be encountered in larger fusion facilities (in TOKAMAK and in other plasma devices as well as accelerators) [1–3].

On the other hand, a new generation of low energy, fast, and compact plasma foci are attracting increasing interest for their potential applications and portability as neutron and X-ray sources [4]. Comparing with isotopic neutron sources, plasma focus devices have unique qualities as sources of X-ray/neutron pulses, emitting only on operator demand, with low risk of radiation contamination and low cost of operation and maintenance. Plasma focus devices are also interesting for industrial applications, ranging from tailored soft X-ray sources, and soft X-ray microlithography to hard X-ray introspective imaging of metallic pieces, neutron production and applications detection of substances, plasma thrusters, materials testing, nanotechnologies, among others [5–26]. Faraday Cup is used to estimate

the ion energy flux with various working nitrogen gas pressures in the chamber of plasma focus device. The results showed that the ion energy flux is associated with the focusing efficiency of plasma focus device as well as working gas pressures [27]. Hassan et al. [28] reported the synthesis of titanium nitride coating on a titanium substrate by utilizing energetic nitrogen ions emitted from a 2.3 kJ dense plasma focus device for 30 focus shots. The corresponding energy flux delivered to the titanium surface was estimated to be 6.17×10^{14} keV cm^{-3} ns^{-1} leading to a transient temperature rise of the top layer of about 5400 K which helps layer growth. Mohanty et al. [29] investigated the pulsed nitrogen ion beams of a 2.2 kJ Mather type plasma focus device with time of flight measurements and revealed that the energy of the ion beams ranged between $\sim$5 to $\sim$700 keV, with the most probable energy of $\sim$25 keV. The ion flux was found strongly dependent on the filling gas pressure. Pulsed ion implantation of nitrogen into pure titanium was studied by Feugeas et al. [30] by employing high current, short length (300 and 400 ns) ion beam pulses. They found that total accumulated ion fluences of 7×10^{14} and 7×10^{16} cm^{-2} showed a heating effect with significant compositional and physical changes in the near surface region of the titanium samples. Sanchez et al. [31, 32] investigated the thermal effect of ion implantation into pure titanium, stainless steel and copper with ultra-short duration ion beams by employing a plasma focus. The PF devices have been operated at capacitor bank energies ranging from tens of Joule to Mega-Joule with different gases. Typical ion fluences produced in the plasma focus devices are 10^{18}–10^{20} ions/m^2 for 100 of ns to a few μs time duration. The energy of ions varies from a few hundreds of eV to MeV and the mean energy of ions is around 100 keV depending on the operation and geometrical parameters of the plasma focus devices [33, 34].

The 11.5 kJ plasma focus device was used here to irradiate materials with fusion grade plasma. The surface modifications of different materials (W, Ni, stainless steel, Mo and Cu) were investigated using various available techniques [35]. Bhuyan et al. [36] have studied the effect of proton irradiations on the tungsten sample in a 2.2 kJ PF device. Batra et al. [37], have studied the low and high energy deuterium ions emission from 4.7 kJ plasma focus device versus pressure using Faraday Cup. This study shows that the ratio of higher energy ions flux to lower energy ions flux increases with lowering the pressure and could be attributed to anomalous resistance in plasma focus device. Lim et al. [38], reported that a 3 kJ Mather type plasma focus system filled with deuterium gas is operated at pressure of 0.05–0.5 mbar. Deuteron beam energy is measured by time of flight technique using three biased ion collectors. The ion beam energy variation with the filling pressure is investigated. Deuteron beam of up to 170 keV are obtained with the strongest deuteron beam measured at 0.1 mbar, with an average energy of 80 keV. The total number of deuterons per shot is in the order of 10^{18} cm^{-2}. Sadowski et al. [39] has shown that the angular distribution of ion emission was similar regardless of the energy of the plasma focus system. Deuteron of >100 keV has been measured at the end-on angle from the 3.6 to 200 kJ plasma focus discharge. Deuteron beam emission was also found to be significant in 3 kJ plasma focus discharge measured by using a deuterated target [40] which also demonstrated that the plasma focus neutron yield is predominantly beam-gas target rather than thermonuclear. The deuterated target enhances the neutron emission through beam target interaction. The ion beam emission from the plasma focus also correlates to the neutron and hard X-ray emission [41], while the different groups of ion beams could correlate to different groups of neutron emission [42, 43]. Gribkov et al. [44] reported that Austenitic steel 10Cr12Mn14Ni4AlMo and Ti-4Al-3V alloy were irradiated with nanosecond pulsed nitrogen ion and plasma streams in plasma focus devices. Two different modes of the treatment were applied: high power density ($\geq 10^{12}$ Wm^{-2}) irradiation with melting of the surface layer and irradiation with power density $\sim 10^{11}$ Wm^{-2} below the melting threshold. It can be said that measurements of ion beams from plasma focus have produced a wide variety of results using different units, often less correlated than expected, and not giving any discernible pattern or benchmark. The Lee model has been modified based on the virtual plasma diode mechanism proposed by Gribkov et al. [45] and [46, 47] for studying of ion beams from plasma focus [48–54].

In this paper, we would like to present and discuss in some detail the results of many numerical calculations carried out using modified Lee model code on different plasma focus devices operated with deuterium for studying of ion beam properties and its comparison with the measured available results for different distances from the anode top.

Properties of Ion Beams Emitted from Plasma Focus

The ion beam exits the plasma focus pinch along its axis. It is a narrow beam (having the same cross-section as the pinch) with little divergence; at least until it overtakes the post-pinch axial shock wave. Hence, the exit beam is best characterized by the ion number per unit cross-section which we term the fluence. Following Lee and Saw [48, 49] we use the following equations:

$$\text{Flux}\ \left(\text{ions m}^{-2}\text{s}^{-1}\right) = \text{J}_\text{b} = 2.75 \times 10^{15} \left(\text{f}_\text{e} \Big/ \left[\text{M Z}_\text{eff}\right]^{1/2}\right) \left\{\left(\ln\left[\text{b}/\text{r}_\text{p}\right]\right) \Big/ \left(r_p^2\right)\right\} \left(\text{I}_\text{pinch}^2\right) \Big/ \text{U}^{1/2} \quad (1)$$

$$\text{Fluence}\ \left(\text{ions m}^{-2}\right) = 2.75 \times 10^{15} \tau \left(\text{f}_\text{e} \Big/ \left[\text{M Z}_\text{eff}\right]^{1/2}\right) \left\{\left(\ln\left[\text{b}/\text{r}_\text{p}\right]\right) \Big/ \left(r_p^2\right)\right\} \left(\text{I}_\text{pinch}^2\right) \Big/ \text{U}^{1/2} \quad (2)$$

where M = mass number of the ion (2 for deuteron), cathode radius b and $f_e = 0.14$ (the fraction of energy converted from pinch inductive energy PIE into beam kinetic energy BKE) is equivalent to ion beam energy of 3–6 % E_0 for cases when the PIE holds 20–40 % of E_0 as observed for low inductance PF. The diode voltage U is $U = 3V_{max}$ taken from data fitting in extensive earlier numerical calculations [55], where V_{max} is the maximum induced voltage of the pre-pinch radial phase.

The value of the ion flux is deduced in each situation for specific machine using specific gas by computing the values of effective charge Z_{eff}, pinch radius r_p, pinch duration τ, pinch current I_{pinch} and U by configuring the Lee Model code with the parameters of the specific machine and specific gas. Once the flux is determined, the following quantities are also computed: power flow density (Wm^{-2}), current density (Am^{-2}), current (A), ions per sec (ions s^{-1}), fluence (ions m^{-2}), number of ions in beam (ions), energy in beam (J), damage Factor ($Wm^{-2}\ s^{0.5}$), energy of fast plasma stream (J). Experimentally it is found that as the focus pinch starts to break up a fast shock wave exits the plasma focus pinch in the axial direction preceding the ion beams which rapidly catches up and overtakes it [45, 49]. Associated with this fast post-pinch axial shock wave is a fast plasma stream (FPS). We estimate the energy of the FPS by computing the work done by the magnetic piston through the whole radial phase from which is subtracted twice the ion beam energy (the second count being for the oppositely directed relativistic electron beam) and from which is further subtracted the radiation yield of the plasma pinch [49]. We also need to emphasize that the calculations of this work pertain to the ion beam at the exit of the pinch. At a distance from the pinch, the propagating ion beam will be attenuated by interaction with the medium traversed and also by beam and stream divergence. The practical importance of these attenuation effects demands further study.

Procedure Used in the Numerical Calculations

The Lee Model code [54–56] is configured to work as any plasma focus by inputting the bank parameters, L_0, C_0 and stray circuit resistance r_0; the tube parameters b, a and z_0 and operational parameters V_0 and p_0 and the fill gas. The standard practice is to fit the computed total current waveform to an experimentally measured total current waveform using four model parameters representing the mass swept-up factor f_m, the plasma current factor f_c for the axial phase and factors f_{mr} and f_{cr} for the radial phases.

From experience it is known that the current trace of the focus is one of the best indicators of gross performance. The axial and radial phase dynamics and the crucial energy transfer into the focus pinch are among the important information that is quickly apparent from the current trace. The exact time profile of the total current trace is governed by the bank parameters, by the focus tube geometry and the operational parameters. It also depends on the fraction of mass swept-up and the fraction of sheath current and the variation of these fractions through the axial and radial phases. These parameters determine the axial and radial dynamics, specifically the axial and radial speeds which in turn affect the profile and magnitudes of the discharge current. The detailed profile of the discharge current during the pinch phase also reflects the Joule heating and radiative yields. At the end of the pinch phase the total current profile also reflects the sudden transition of the current flow from a constricted pinch to a large column flow. Thus the discharge current powers all dynamic, electrodynamics, thermodynamic and radiation processes in the various phases of the plasma focus. Conversely all the dynamic, electrodynamics, thermodynamic and radiation processes in the various phases of the plasma focus affect the discharge current. It is then no exaggeration to say that the discharge current waveform contains information on all the dynamic, electrodynamics, thermodynamic and radiation processes that occurs in the various phases of the plasma focus. This explains the importance attached to matching the computed current trace to the measured current trace in the procedure adopted by the Lee Model code.

Numerical Calculations: Results and Discussion

Soto et al. [57] had published a paper with laboratory measurements from the PF-400J, including a typical current waveform and a characterization of plasma bursts produced after the pinch phase in a plasma focus of hundreds of joules, using pulsed optical refractive techniques. We first fit the computed current waveform to the published measured waveform in the following manner.

We then configure the Lee model code (version RADPF5.15 FIB) to operate as the PF-400J starting with the following published [57] bank and tube parameters:

Bank parameters: $L_0 = 38\,\text{nH}, C_0 = 0.88\,\mu\text{F}, r_0 = \text{not given}$

Tube parameters: $b = 1.55\,\text{cm}, a = 0.6\,\text{cm}, z_0 = 2.8\,\text{cm}$

Operating parameters: $V_0 = 28\,\text{kV}$, $p_0 = 6.75\,\text{Torr Deuterium}$

where L_0 = static inductance (nominal), C_0 = storage capacitance (nominal), b = tube outer radius, a = inner radius, z_0 = tube axial length, V_0 = operating voltage, p_0 = operating initial pressure.

The computed total current waveform is fitted to a measured waveform by varying model parameters f_m, f_c, f_{mr} and f_{cr} sequentially, until the computed waveform agrees with the measured waveform. First, the axial model factors f_m, f_c are adjusted (fitted) until the features (a) computed rising slope of the total current trace and (b) the rounding off of the peak current as well as (c) the peak current itself are in reasonable (typically very good) fit with the measured total current trace. Then the radial phase model factors f_{mr} and f_{cr} are adjusted sequentially until (d) the computed slope of the current dip and (e) the depth of the dip agree with the measured. Once fitted the code outputs in tabular and graphical forms realistic data of the following: axial and radial dynamics (positions and speeds), pinch length and minimum pinch radius, temperatures and densities, Bremsstrahlung and line yields, thermonuclear and beam-target neutron yields, fast ion beam flux and fluence, energy flux and fluence, power flow and damage factors, fast plasma stream energies and speeds [56].

To obtain a reasonably good fit the following bank and tube parameters (L_0, C_0 and z_0 fitted and r_0 fitted) are used:

Bank parameters: $L_0 = 40$ nH, $C_0 = 0.95$ μF, $r_0 = 10$ mΩ

Tube parameters: b = 1.55 cm, $a = 0.6$ cm, $z_0 = 1.7$ cm

Operating parameters: $V_0 = 28$ kV, $P_0 = 6.75$ Torr Deuterium

together with the following fitted model parameters:

$f_m = 0.08$, $f_c = 0.7$, $f_{mr} = 0.11$ and $f_{cr} = 0.7$.

The fitted computed current waveform is compared with published waveform in Fig. 1.

These fitted values of the model parameters are then used for the computation of all the discharges at various pressures. The numerical calculations using Lee model at the bank and tube parameters last mentioned above and using the fitted model parameters give the following results: the end axial speed $v_a = 9$ cm/μs, the speed factor $SF = (I_0/ap_0^{1/2})$ is 81 kA/cm per [Torr of Deuterium]$^{1/2}$. The plasma parameters (dimensions, speeds) are changing slowly in the first half part of the inward shock phase. The final plasma column is 0.09 cm in radius, and 0.8 cm in length. The inward shock speed is steadily increasing in the inward shock phase to a final on-axis speed of $V_s = 33$ cm/μs and the radial piston speed is also increasing to a maximum value of $V_p = 22.5$ cm/μs and

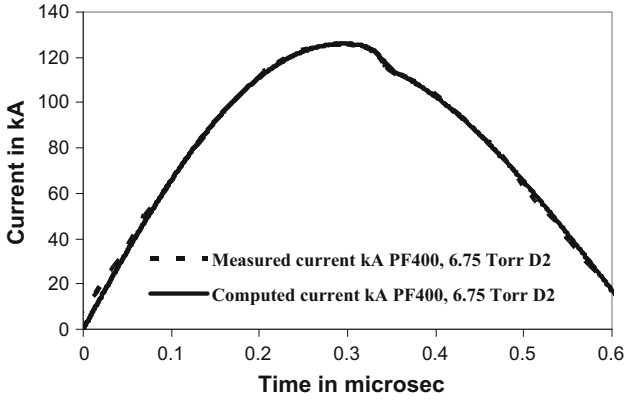

Fig. 1 Computed discharge current compared to published current for PF-400 J

the pinch duration is about 5.3 ns [56]. The average radial speed on the whole radial trajectory is about 12 cm/μs. At these conditions the neutron yield Y_n emitted from Deuterium plasma focus is computed as 1.03×10^6. The peak values of total discharge current I_{peak} is 126 kA, the pinch current I_{pinch} is 81 kA, and the focusing time (time at focus from start of discharge) is 0.35 μs. The focusing time increases with increase in the gas pressure, while it decreases with increase in the charging voltage. This can be ascribed to the increase in energy pumping to plasma focus which causing an increase in the current sheath velocity in both axial and radial phases before forming focus. These fitted values of the model parameters are then used for the computation of all the discharges at various pressures, fixing all the mentioned above parameters. From obtained results, it is seen that the Y_n increases with increasing pressure until it reaches the maximum value about 1.17×10^6 at $p_0 = 5$ Torr, after which it decreases with higher pressures and it is compared with the published values $(1.2 \pm 0.2) \times 10^6$ [57] (more detailed numerical calculations on PF-400J neutron yield versus pressure are carried out, and found to compare well with laboratory experiments. These have already been published in [58]).

Soto et al. [57] showed that the plasma in the PF-400J at 6.75 Torr is compressed with a speed of the order (8 ± 0.8) cm/μs forming a pinch plasma column with a radius of (0.1 ± 0.015) cm, and length ~0.6 cm. These experimental results compare well with the numerical results obtained by Lee model at the same conditions; these simulated results being: The average radial speed = 12 cm/μs, the pinch radius = 0.09 cm, the pinch length = 0.8 cm.

We continue our numerical calculations for studying the ion beam properties (ion beam energy, ion beam flux, ion beam fluence, beam ion number, ion beam current, power flow density, and damage factor) emitted from PF-400J

versus gas pressure. The numerical calculations using the modified Lee model give the following results at an operating pressure of 6.75 Torr: Ion fluence = 1.67×10^{20} - m^{-2}, the ion flux = 3.15×10^{28} m^{-2} s^{-1}, the ion energy is 50 keV, the ion number is 3.9×10^{14}, the beam energy is 3.1 J, the energy of the fast plasma stream (FPS) is 19 J, the FPS speed is 33 cm/μs, the power flow density of the streams is 2.5×10^{14} Wm^{-2}, the Damage factor 1.82×10^{10} Wm^{-2} $s^{0.5}$. Soto et al. [57] have characterized the axial plasma shock in the PF-400J operated with 6.75 Torr deuterium during the pinch formation and after the pinch ejection. They used Schlieren imaging. They showed that while the pinch is ejected, a secondary axial plasma structure (bubble) intersecting the primary plasma appears and three different fronts are identified in the plasma structure (Z_1 indicates the rear of the axial plasma sheath, Z_2 is the front of the plasma sheath, and Z_3 is the axial front of a plasma bubble that appears after the pinch) (see Fig. 2). The obtained experimental results at 6.75 Torr are: the axial velocity of the bubble front Z_3 (or the fast plasma stream FPS) is about 30 cm/μs and the maximum measured FPS Energy is 16 J. These results are in reasonable agreement compared to our numerical results at the same operational parameters. Our computed results being: FPS speed of 33 cm/μs and the energy of the fast plasma stream (FPS) is 19 J.

For studying the effect of pressure on the ion beam characteristics, more numerical calculations were carried out with the above model parameters; but varying pressure from 1 to 14 Torr (see Table 1).

Table 1 shows that the ion flux initially increases with the increase in gas pressure and reaches a maximum (3.15×10^{28} ions m^{-2} s^{-1}) at a pressure of 6.75 Torr. The

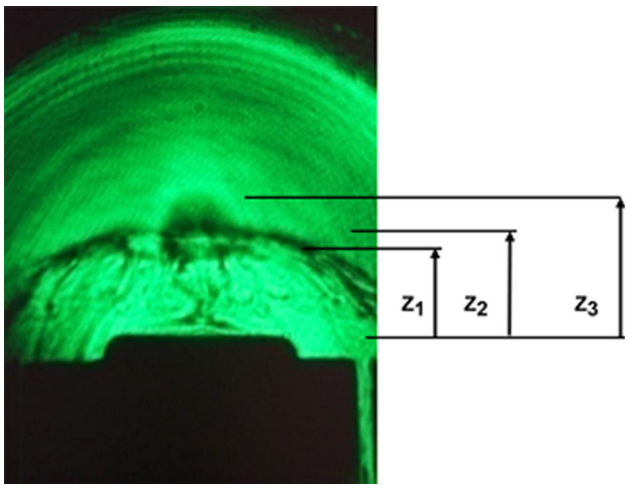

Fig. 2 Different fronts identified in the plasma structure. Z_1 indicates the rear of the axial plasma sheath, Z_2 is the front of the plasma sheath, and Z_3 is the axial front of a plasma bubble that appears after the pinch [taken from ref. 57]

beam ion number increases with the increase in gas pressure until the plasma pinch becomes very weak. The beam ion number range from about 9.4×10^{13} to 6.6×10^{14} for PF-400J. Plasma focus devices have three typical regimes of influence of ion and plasma beams upon a target material placed downstream of the pinch [46, 59, 60]: (1) "implantation mode" of irradiation when power flow density of the streams is (10^9–10^{11} Wm^{-2}) (2) screening of the surface by a secondary plasma cloud in the so-called "detachment mode" ($\approx 10^{11}$–10^{12} Wm^{-2}) (3) strong damage with the absence of implantation in the "explosive destruction mode" ($\approx 10^{12}$–10^{14} Wm^{-2}). Numerical calculations using modified Lee model showed that the maximum power flow density reaches almost 3.4×10^{14} Wm^{-2} at a pressure of 3 Torr, and decreases with higher pressures. So, based on the obtained power flow densities, it can be said that the explosive destruction mode is dominant for the PF-400J operation at the pinch exit position. The damage factor is defined as power flow density multiplied by (pulse duration)$^{0.5}$. It is shown that, the damage factor reaches almost 2×10^{10} Wm^{-2} $s^{0.5}$ for PF-400J at a pressure of 4 Torr. These above mentioned calculations of this work pertain to the ion beam at the exit of the formed pinch. Generally, as distance increases from the pinch to the target, the propagating ion beam will be attenuated by interaction with the medium traversed and also by beam and stream divergence. In our calculations, the energy loss for energetic ions due to interactions with the background gas (deuterium) is too low to be considered at small distances and is neglected (For example, the energy loss of a 100 keV deuteron passing of deuterium gas with 5 Torr pressure is about 1 keV/cm and it is even less for higher energy deuterons [61]). Furthermore, to factor in beam and stream divergence, for simplicity in our calculations, we considered an ion beam with conic geometry with a full angles of 40–60° [31, 32, 62, 63]. Based on these above mentioned conditions and Lee model results, we proceed to estimate the ion beam properties at different distances from the pinch using the following relation for ion beam fluence [31, 32]:

$f_i = \frac{N_i}{\sigma_R}$, where N_i ion number (taken from Lee model), $\sigma_R = \pi(R \tan\theta)^2$—is the cross section of the beam at a R distance from the focus, θ—half angle of the emission. From their experimental results, Soto et al. [57] showed that the cross section of the stream is about 2 cm^2 for target located at 1.5 cm from the anode top, and that the power flow density or energy flux (energy per unit area per second) and integral damage factor are 1.25×10^{12} Wm^{-2} and 1.8×10^8 Wm^{-2} $s^{0.5}$, respectively. So, we proceed our numerical calculations to compare with the experiments on PF-400J. We took the half angle as 30° and obtain the results tabulated in the Table 2.

Table 1 Variation of ion beam properties emitted from PF-400 J at the pinch exit

P_0 (Torr)	Fluence ($\times 10^{20}$ ions m^{-2})	Flux ($\times 10^{28}$ ions m^{-2} s^{-1})	Power flow density ($\times 10^{14}$ Wm^{-2})	Damage factor ($\times 10^{10}$ Wm^{-2} $s^{0.5}$)	IB En (J)	FPS En (J)	FPS speed (cm/μs)	Ion number ($\times 10^{14}$)
1.00	0.44	1.89	3.0	1.46	1.49	14.4	81.9	0.94
2.00	0.73	2.45	3.4	1.84	2.16	17.4	63.4	1.6
3.00	0.98	2.78	3.4	2.00	2.58	18.9	53.4	2.1
4.00	1.19	2.99	3.2	2.03	2.84	19.6	46.5	2.6
5.00	1.39	3.10	3.0	1.99	3.00	19.9	41.1	3.1
6.00	1.56	3.15	2.7	1.91	3.08	19.9	36.8	3.6
6.75	1.67	3.15	2.5	1.82	3.09	19.8	33.9	3.9
7.00	1.71	3.15	2.4	1.78	3.08	19.8	33.1	4.0
8.00	1.84	3.10	2.1	1.64	3.04	19.5	29.8	4.4
9.00	1.95	3.01	1.8	1.48	2.94	19.1	26.9	4.8
10.00	2.04	2.88	1.5	1.31	2.81	18.6	24.1	5.2
12.00	2.13	2.51	1.0	0.95	2.46	17.5	19.2	6.0
14.00	2.05	1.99	0.6	0.61	1.99	16.4	14.6	6.6

Table 2 Variation of ion beam properties emitted from PF-400 J at different distances for 6.75 Torr D_2

R (cm)	Fluence ($\times 10^{18}$ ions m^{-2})	Flux ($\times 10^{26}$ ions m^{-2} s^{-1})	Power flow density ($\times 10^{12}$ Wm^{-2})	Damage factor ($\times 10^{8}$ Wm^{-2} $s^{0.5}$)
In the pinch	167	310	250	180
1	3.73	7.03	5.52	4.02
1.5	1.65	3.12	2.45	1.78
2	0.93	1.75	1.38	1.00
3	0.4	0.78	0.6	0.45
4	0.23	0.44	0.34	0.25
5	0.15	0.28	0.22	0.16
6	0.1	0.2	0.15	0.11
7	0.07	0.14	0.11	0.082
8	0.06	0.11	0.09	0.063
9	0.046	0.09	0.07	0.05

From the table, it is noticed that the for material target located at 1.5 cm from the anode top, the power flow density (or energy flux) and integral damage factor are 2.45×10^{12} Wm^{-2} ($\sim$2 times of experimental value) and 1.78×10^{8} Wm^{-2} $s^{0.5}$ ($\sim$almost the same as experimental value), respectively. These comparisons give the numerical results by Lee model more credibility for studying of the ion beam properties emitted from plasma focus.

The above mentioned measured and numerical results on PF-400J are tabulated for a comparative study as shown in the Table 3.

Additional numerical calculations have been also carried out on the other plasma focus devices operated with deuterium (PF50 [4], NX2, NX3, FMPF-3 [64], 2.2 kJ PF [65], INTI PF [48]) for ion beam study at the pinch exit and different distances from the anode top.

Our numerical calculations confirm that even though the lifetime of the pinch [66] hence the time interaction of the plasma produced by plasma focus devices is orders of magnitude shorter than conventional beam generators used in radiation material tests (for example electron and ion beams generators and accelerators), the power flux density is orders of magnitude higher than those instruments. In these conditions, many features of damage produced by plasma blasts, taking place in relatively long events, could be reproduced with small plasma focus devices. In particular, in the TOKAMAKS (projected tokamak ITER), the power flow density $\sim 10^{10}$ Wm^{-2} and integral damage factor $\sim 10^{8}$ Wm^{-2} $s^{0.5}$ are expected from type I ELMs (edge localized modes) [57]. Therefore, the information obtained from these numerical calculations and experiments on the plasma focus PF-400J, or similar small

Table 3 Measured and computed ion beam properties of PF-400 J operated with deuterium

PF-400 J	Measured	Computed
pressure (Torr)	6.75	6.75
I_{peak} (kA)	130	126
z_p (cm)	0.6	0.8
r_p (cm)	(0.1 ± 0.015)	0.09
Average radial speed (cm/μs)	(8 ± 0.8)	12
FPS speed (cm/μs)	30	33
FPS energy (J)	16	19
Power flow density ($\times 10^{12}$ Wm^{-2})	1.25	2.45
Damage factor ($\times 10^{8}$ Wm^{-2} $s^{0.5}$)	1.8	1.78
Maximum neutron yield	(1.2 ± 0.2) × 10^6	1.17 × 10^6

plasma focus devices (PF50, NX2, NX3, FMPF-3, INTI PF), are useful to study the effects of fusion-relevant cumulative pulses on target materials. For this application, the target should be located close to the end of the pinch, where the damage factor is of the order of $\sim 10^8$ Wm^{-2} $s^{0.5}$ (i.e., as near as possible without affecting the initiation of the discharge and the radial plasma focus dynamics). In a plasma focus device, the damage factor could be tuned by adjusting the distance of the target from the focus pinch. In addition, exposure frequencies of 1 Hz or greater can be obtained in small plasma focus devices and thousand shots can be produced in a few minutes [67]. Therefore, important progress could be achieved in materials damage testing for fusion reactors using small plasma focus devices as plasma sources.

Conclusion

The modified Lee model code has been used to study ion beam properties of plasma focus with deuterium filling gas. Many numerical calculations were carried out in different plasma focus devices. The variation of ion beams versus pressure for different plasma focus parameters have been studied. The numerical calculations using the modified Lee model on PF-400J at the 6.75 Torr of deuterium give the following results: Ion fluence = 1.67 × 10^{20} m^{-2}, the ion flux = 3.15 × 10^{28} m^{-2} s^{-1}, the ion energy is 50 keV, the ion number is 3.9 × 10^{14}, the beam energy is 3.1 J, the energy of the fast plasma stream (FPS) is 19 J, the FPS speed is 33 cm/μs, the power flow density of the streams is 2.5 × 10^{14} Wm^{-2}, the Damage factor 1.82 × 10^{10} Wm^{-2} $s^{0.5}$. The computed ion beam properties of PF-400J are in reasonable agreement with reported measured values. For example the energy flux and integral damage factor are computed as 2.45 × 10^{12} Wm^{-2} (∼2 times of experimental value) and 1.78 × 10^8 $Wm^{-2}s^{0.5}$ (∼almost the same experimental value) respectively, for material target located at 1.5 cm from the anode top of PF-400J. Our numerical results confirm that the low energy plasma focus devices could be a good tool for plasma surface interaction study related to plasma-exposed walls of Tokamak fusion reactors. It has already been established that the fluence and flux and energy fluence and flux and damage factors have similar values within a narrow range for all plasma focus whether big or small [48, 49]. Thus small plasma focus devices can produce as much damage as a big plasma focus; except that the damage produced in a small plasma focus is over a smaller area compared to the bigger target area that the big plasma focus can irradiate on a per shot basis. However, exposure frequencies of 1 Hz or greater can be obtained in small plasma focus devices achieving thousands of shots in a few minutes. Thus the damage accumulated over a number of shots can be achieved much more rapidly in a small plasma focus fired repetitively than in a big focus which is single shot. Therefore, important progress could be achieved in materials damage testing for plasma facing walls of fusion reactors using small plasma focus devices as plasma sources.

Acknowledgments The authors would like to thank Director General of AECS, for encouragement and permanent support. SHS and SL would like to acknowledge IAEA Research Contract: 16934 of CRP F1.30.13 and FRGS/2/2013/SG02/INTI/01/1.

References

1. V.A. Gribkov, B. Bienkowska, M. Borowiecki, A.V. Dubrovsky, I. Ivanova-Stanik, L. Karpinski, R.A. Miklaszewski, M. Paduch, M. Scholz, K. Tomaszewski, J. Phys. D Appl. Phys. **40**, 1977 (2007)
2. A. Cicuttin, M.L. Crespo, V.A. Gribkov, J. Niemela, C. Tuniz, C. Zanolli, M. Chernyshova, E.V. Demina, S.V. Latyshev, V.N. Pimenov, A.A. Talab, Nucl. Fusion **55**, 063037 (2015)
3. M.J. Inestrosa-Izurieta, E. Ramos-Moore, L. Soto, Nucl. Fusion **55**, 093011 (2015)
4. A. Clausse, L. Soto, A. Tarifeño-Saldivia, IEEE Trans. Plasma Sci. **43**(2), 629 (2015)
5. K.S. Tan, R.J. Mah, R.S. Rawat, IEEE Trans. Plasma Sci. **43**, 2539 (2015)

6. I.A. Khan, M. Hassan, T. Hussain, R. Ahmad, M. Zakaullah, R.S. Rawat, Appl. Surf. Sci. **255**, 6132 (2009)
7. I.A. Khan, S. Jabbar, T. Hussain, M. Hassan, R. Ahmad, M. Zakaullah, Nucl. Instrum. Methods Phy. Res. B **268**, 2228 (2010)
8. T. Hussain, R. Ahmad, I.A. Khan, J. Siddiqui, N. Khalid, A.S. Bhatti, Nucl Naseem, Instrum. Methods Phys. Res. B **267**, 768 (2009)
9. S. Jabbar, I.A. Khan, R. Ahmad, M. Zakaullah, J.S. Pan, J. Vac. Sci. Technol. A **27**(2), 381 (2009)
10. M. Sadiq, S. Ahmad, M. Shafiq, M. Zakaullah, Nucl. Instrum. Methods Phys. Res. B **252**, 219 (2006)
11. R.S. Rawat, W.M. Chew, P. Lee, T. White, S. Lee, Surf. Coat. Technol. **173**, 276 (2003)
12. M. Hassan, R. Ahmad, A. Qayyum, G. Murtaza, A. Waheed, M. Zakaullah, Vacuum **81**, 291 (2006)
13. M. Hassan, A. Qayyum, R. Ahmad, G. Murtaza, M. Zakaullah, J. Phys. D Appl. Phys. **40**, 769 (2007)
14. S.R. Mohanty, N.K. Neog, H. Bhuyan, R.K. Rout, R.S. Rawat, P. Lee, Jpn. J. Appl. Phys. **46**, 3039 (2007)
15. B.B. Nayak, B.S. Acharya, S.R. Mohanty, T.K. Borthakur, H. Bhuyan, Surf. Coat. Technol. **145**, 15 (2001)
16. J. Feugeas, G. Grigioni, G. Sanches, A.R. DaCosta, Surf. Eng. **14**, 62 (1998)
17. J. Piekoszewski, B. Sartowska, L. Walíś, Z. Werner, M. Kopcewicz, F. Prokert, J. Stanisławski, J. Kalinowska, W. Szymczyk, Nukleonika **49**(2), 57 (2004)
18. M.J. Marques, J. Pina, A.M. Dias, J.L. Lebrun, J. Feugeas, Surf. Coat. Technol. **195**, 8 (2005)
19. H. Kelly, A. Lepone, A. Márquez, D. Lamas, C. Oviedo, Plasma Sources Sci. Technol. **5**, 704 (1996)
20. M. Ahmad, S. Al-Hawat, M. Akel, O. Mrad, J.Appl. Phys. **117**, 063301 (2015)
21. M. Ahmad, S. Al-Hawat, M. Akel, J. Fusion Energ **32**(4), 471 (2013)
22. S. Al-Hawat, M. Soukieh, M. Abou Kharoub, W. Al-Sadat, Vacuum **84**, 907 (2010)
23. J. Siddiqui, T. Hussain, R. Ahmad, W. Ali, A. Hussnain, R. Ayub, J. Fusion Energ. (2015). doi:10.1007/s10894-015-9943-2
24. J. Siddiqui, T. Hussain, R. Ahmad, N. Khalid, Chin. Phys. B **24**(6), 065204 (2015)
25. M.T. Hosseinnejad, Z. Ghorannevis, M. Ghoranneviss, G. Reza Etaati, M. Shirazi, J. Fusion Energ. **34**(6), 1217–1228 (2015)
26. R.S. Rawat, Dense plasma focus—from alternative fusion source to versatile high energy density plasma source for plasma nanotechnology. J. Phys: Conf. Ser. **591**, 012021 (2015)
27. H.A.R. Tariq, I.A. Khan, U. Ikhlaq, A. Hussnain, J. Nat. Sci. Maths. **48**(12), 65 (2008)
28. M. Hassan, A. Qayyum, R. Ahmad, R.S. Rawat, P. Lee, S.M. Hassan, G. Murtaza, M. Zakaullah, Nucl. Instrum. Methods Phys. Res. B **267**, 1911 (2009)
29. S.R. Mohanty, H. Bhuyan, N.K. Neog, R.K. Rout, E. Hotta, Jpn. J. Appl. Phys. **44**(7A), 5199 (2005)
30. J.N. Feugeas, C.O. de Gonzalez, G. Sanchez, Radiat. Eff. Defects Solids **128**, 267 (1994)
31. G. Sanchez, G. Grigioni, J. Feugeas, Surf. Coat. Technol. **70**, 181 (1995)
32. G. Sanchez, J. Feugeas, J. Pys, D Appl. Phys. **30**, 927 (1997)
33. R.A. Behbahani, F.M. Aghamir, J. Appl. Phys. **111**, 043304–043305 (2012)
34. H. Bhuyan, H. Chuaqui, M. Favre, I. Mitchell, E. Wyndham, J. Phys. D Appl. Phys. **38**, 1164–1169 (2005)
35. R. Niranjan, R.K. Rout, R. Srivastava, Y. Chakravarthy, P. Mishra, T.C. Kaushik, S.C. Gupta, Appl. Surf. Sci. **355**, 989 (2015)
36. M. Bhuyan, S.R. Mohanty, C.V.S. Rao, P.A. Rayjada, P.M. Raole, Appl. Surf. Sci. **264**, 674 (2013)
37. J. Batra, A. Jaiswar, R. Srivastava, R. Niranjan, R.K. Rout, T.C. Kaushik, Indian J. Pure Appl. Phys. **25**, 246 (2014)
38. L.K. Lim, S.L. Yap, C.S. Wong, M. Zakaullah, J. Fusion Energ. **32**(2), 287–292 (2013)
39. M. Sadowski, J. Zebrowski, E. Rydygier, J. Kucinski, Plasma Phys. Control Fusion **30**(6), 763–769 (1988)
40. S.P. Moo, C.K. Chakrabarty, S. Lee, I.E.E.E. Trans, Plasma Sci. **19**(3), 515–519 (1991)
41. H. Kelly, A. Márquez, Plasma Phys. Control Fusion **38**(11), 1931–1942 (1996)
42. S.L. Yap, C.S. Wong, P. Choi, C. Dumitrescu, S.P. Moo, Jpn. J. Appl. Phys. **44**(11), 8125–8132 (2005)
43. H. Schmidt, P. Kubes, M.J. Sadowski, M. Scholz, I.E.E.E. Trans, Plasma Sci. **34**(5III), 2363–2367 (2006)
44. V.A. Gribkov, V.N. Pimenov, V.V. Roschupkin, S.A. Maslyaev, E.V. Demina, M.M. Lyakhovitsky, A.V. Dubrovsky, I.P. Sasinovskaya, M. Chernyshova, M. Scholz, M.L. Crespo, A. Chicutin, Claudio Tuniz Nukleonika **57**, 291 (2012)
45. V.A. Gribkov, A. Banaszak, B. Bienkowska, A.V. Dubrovsky, I. Ivanova-Stanik, L. Jakubowski, L. Karpinski, R.A. Miklaszewski, M. Paduch, M.J. Sadowski, M. Scholz, A. Szydlowski, K. Tomaszewski, J. Phys. D Appl. Phys. **40**, 3592 (2007)
46. V.N. Pimenov, E.V. Demina, S.A. Maslyaev, L.I. Ivanov, V.A. Gribkov, A.V. Dubrovsky, Ü. Ugaste, T. Laas, M. Scholz, R. Miklaszewski, B. Kolman, A. Tartari, Nukleonika **53**(3), 111–121 (2008)
47. V.A. Gribkov, Plasma Phys. Controll. Fusion **57**, 065010 (2015)
48. S. Lee, S.H. Saw, Phys. Plasmas **19**, 112703 (2012)
49. S. Lee, S.H. Saw, Phys. Plasmas **20**, 062702 (2013)
50. M. Akel, S. Alsheikh Salo, S.H. Saw, S. Lee, J. Fusion Energ. **33**(2), 189–197 (2014)
51. M. Akel, S. Alsheikh Salo, S.H. Saw, S. Lee, Vacuum **110**, 54–57 (2014)
52. M. Akel, S. Alsheikh Salo, S.H. Saw, S. Lee, IEEE Trans. Plasma Sci. **42**(9), 2202–2206 (2014)
53. M. Akel, S. Alsheikh Salo, S. Ismael, S.H. Saw, S. Lee, Phys. Plasmas **21**, 072507 (2014)
54. Lee S, http://www.plasmafocus.net (2015)
55. S. Lee, S.H. Saw, J. Fusion Energ. **27**, 292–295 (2008)
56. S. Lee, J. Fusion Energ. **33**(4), 319–335 (2014)
57. L. Soto, C. Pavez, J. Moreno, M.J. Inestrosa-Izurieta, F. Veloso, G. Gutierrez, J. Vergara, A. Clausse, H. Bruzzone, F. Castillo, L.F. Delgado-Aparicio, Phys. Plasmas **21**, 122703 (2014)
58. S. Lee, S.H. Saw, L. Soto, S.V. Springham, S.P. Moo, Plasma Phys. Control. Fusion **51**, 075006 (2009)
59. V.A. Gribkov, V.N. Pimenov, L.I. Ivanov, E.V. Dyomina, S.A. Maslyaev, R. Miklaszewski, M. Scholz, U.E. Ugaste, A.V. Dubrovsky, V.C. Kulikauskas, V.V. Zatekin, J. Phys. D Appl. Phys. **36**, 1817–1825 (2003)
60. V.N. Pimenov, S.A. Maslyaev, L.I. Ivanov, E.V. Dyomina, V.A. Gribkov, A.V. Dubrovsky, M. Scholz, R. Miklaszewski, U.E. Ugaste, B. Kolman, Nukleonika **51**, 71 (2006)
61. See online available: http://www.srim.org (SRIM-2013 for the Stopping and Range of Ions in Matter)
62. M. Sohrabi, M. Habibi, H.R. Yousefi, G.H. Roshani, Contrib. Plasma Phys. **53**(3), 592–598 (2013)
63. M. Habibi, Phys. Lett. A **380**(3), 439–443 (2016)
64. S.H. Saw, P. Lee, R.S. Rawat, R. Verma, D. Subedi, R. Khanal, P. Gautam, R. Shrestha, A. Singh, S. Lee, J. Fusion Energ. **34**(3), 474–479 (2015)
65. N. Talukdar, N.K. Neog, T.K. Borthakur, Phys. Plasmas **21**, 062709 (2014)
66. S. Lee, A. Serban, IEEE Trans. Plasma Sci. **24**, 1101–1105 (1996)
67. S. Lee, P. Lee, G. Zhang, X. Feng, V.A. Gribkov, M. Liu, A. Serban, T. Wong, I.E.E.E. Trans, Plasma Sci. **26**, 1119 (1998)